https://doi.org/10.3311/PPme.21216

Periodica Polytechnica Mechanical Engineering, 66(4), pp. 361–364, 2022

Deformation Induced Lattice Misorientation in Lath Martensite

Péter J. Szabó

[1] Department of Materials Science and Engineering, Faculty of Mechanical Engineering, Budapest University of Technology and Economics, P. O. B. 91, H-1521 Budapest, Hungary
[*] Corresponding author, e-mail: szabo.peter.janos@gpk.bme.hu

Received: 21 September 2022, Accepted: 21 September 2022, Published online: 22 September 2022

Abstract

Effect of plastic deformation on the lattice misorientation in lath martensite was investigated by Electron Backscatter Diffraction (EBSD). As-quenched rod-like specimens were plastically deformed until 9000 N, 14000 N, 19000 N and 21000 N of tensile loading. Grain average misorientation maps were collected by EBSD. It was shown that the average misorientation during plastic deformation increased from 0.887 to 1.156 degrees. Results showed that the density of geometrically necessary dislocations, which caused the lattice misorientation, slightly increased during plastic deformation of lath martensite.

Keywords

lath martensite, Electron Backscatter Diffraction (EBSD), grain average misorientation

1 Introduction

Martensitic steel is one of the most widely used iron base structural materials with the most outstanding mechanical properties. Besides Fe it consists of carbon varying between a few hundredths to a few tenths of weight percent and a variety of different alloying elements, however, also in small quantities. It is produced by fast cooling from a temperature where the fcc austenitic γ phase is stable to around room temperature where the bcc α phase is stable. All physical properties depend on the alloy composition, but first of all on the carbon content and the cooling conditions. Martensitic alloy itself has a history of a few thousand years since carbon is always present in iron and the beneficial strengthening effect was detected at the very first production of iron for usage in daily life. Despite this long history the microstructural operation of martensite is still a puzzle. The strength is evoked by the phase transformation from the fcc γ to the bcc α phase. The speed of cooling from the austenite state and the carbon content are the main factors determining the microstructure and the mechanical properties of martensitic steels [1]. One possible form of martensite is the so-called lath martensite. A typical lath martensite consists of blocks of lamellar plates, where the blocks are forming packets [2–4]. The blocks are further subdivided into sub-blocks, where the smallest constituents of the structure are the lamellar plates called martensite-laths. The hierarchical structure of packets, blocks, sub-blocks and laths in lath martensite is shown schematically in Fig. 1.

The packets are of the same crystallographic orientation in which the 110 type planes align coherently along the 111 type planes of the prior austenite phase, out of which the bcc martensite was formed. Within the prior austenite grain boundary several packets of different crystallographic orientations can coexist [2–4], as shown in Fig. 1. Despite the rather large elastic limit of martensitic steels, they do show some ductility [1, 5–7]. The microscopic mechanism controlling plastic deformation in lath-martensite has recently been attempted to be revealed by

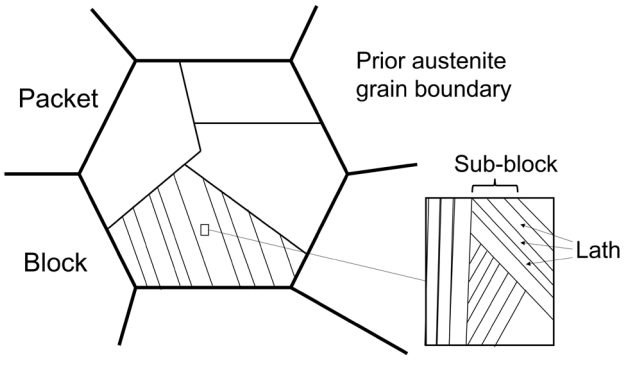

Fig. 1 The hierarchical structure of packets, blocks, sub-blocks and laths in lath martensite

Cite this article as: Szabó, P. J. "Deformation Induced Lattice Misorientation in Lath Martensite", Periodica Polytechnica Mechanical Engineering, 66(4), pp. 361–364, 2022. https://doi.org/10.3311/PPme.21216

microscale deformation experiments [8, 9]. Micropillars with a single martensite block have shown perfectly ideal stress-strain behavior with no strain hardening and a flow stress of 1.2 GPa. Micropillars with two or more blocks, however, have shown significant strain hardening with a similarly large elastic limit [8].

2 Experimental

2.1 Specimens

The composition of the AISI 1015 as-received steel plate was (in weight percentage) 0.13–0.18% carbon (C), 0.30–0.60% manganese (Mn), 0.04%(max) phosphorus (P), 0.05%(max) sulfur (S), and the base metal iron (Fe). The steel rod had no specific texture. The rod was annealed at 1100 °C for 30 minutes and then quenched into room temperature water. After quenching the microstructure of the specimens were fully lath martensitic, as it can be seen in Fig. 2.

From the quenched rod 12 standard tensile specimens were cut for tensile tests. The tensile deformations were carried out in an MTS-810 standard testing machine at the strain velocity of 1 mm/min at room temperature. 3–3 specimens were elongated to maximum force of 9000 N, 14000 N, 19000 N and 21000 N (the latter force arose right before fracture). The averaged tensile force vs. elongation curves are shown in Fig. 3.

The numbers of the specimens and the tensile loading forces belonging to each specimen is shown in Table 1.

Cross sectional specimens were then manufactured from the differently elongated rods in order to perform EBSD measurements. These specimens were ground, and polished by 0.05 mm colloidal silica.

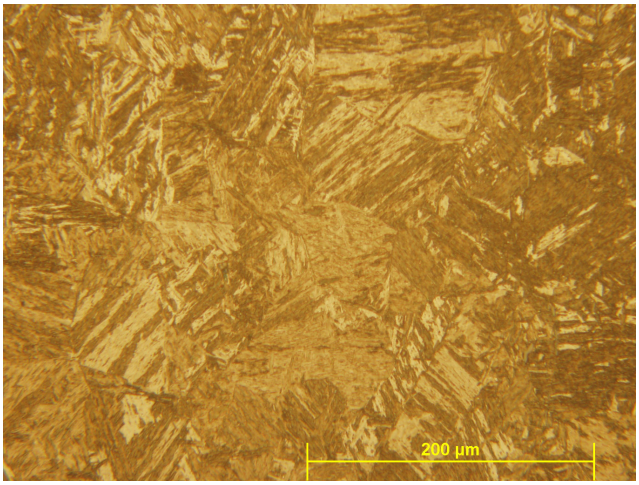

Fig. 2 Optical micrograph taken from the as-quenched specimen

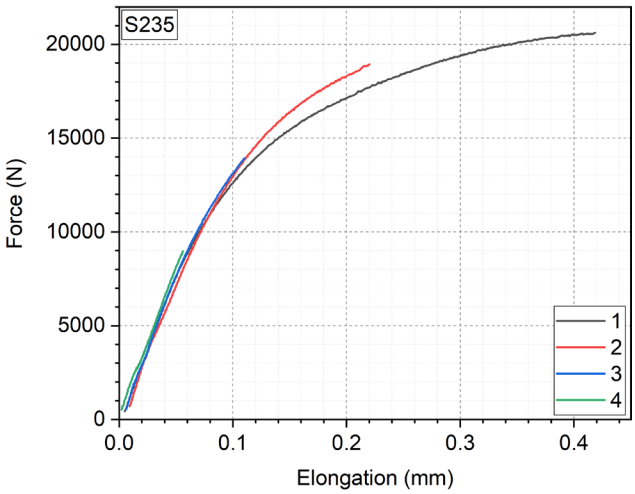

Fig. 3 Average tensile force vs. elongation during tensile loading of lath martensite specimens

Table 1 Tensile force vs. elongation curves of the specimens

Specimen	1	2	3	4
Tensile loading force, N	9000	14000	19000	21000

2.2 EBSD measurements

Electron Backscatter Diffraction (EBSD) measurements were performed on the specimens by a Philips XL-30 scanning electron microscope equipped with an EDAX-TSL EBSD system. Orientation maps were recorded in a scan area of 180 × 120 mm with a step size of 0.8 mm in hexagonal arrangement. Results were evaluated by TSL OIM Analysis software. Grain dilatation clean-up procedure were performed before evaluating the maps.

3 Results

Fig. 4 shows the grain average misorientation maps of the four differently elongated specimens. It should be noted that the color coding of the 4 maps is similar. Grain average misorientation increases from blue to red according to rainbow color coding scheme.

In this mode each point in the grain is shaded the same color in maps of this type. The misorientation between each neighboring pair of points within the grain is calculated. The average misorientation value is then determined and assigned to each point within the grain. The average grain misorientations were calculated for each map, the results are shown in Table 2.

It can well be seen in Fig. 5 that the grain average misorientation shows a monotonic increment with the applied tensile loading force.

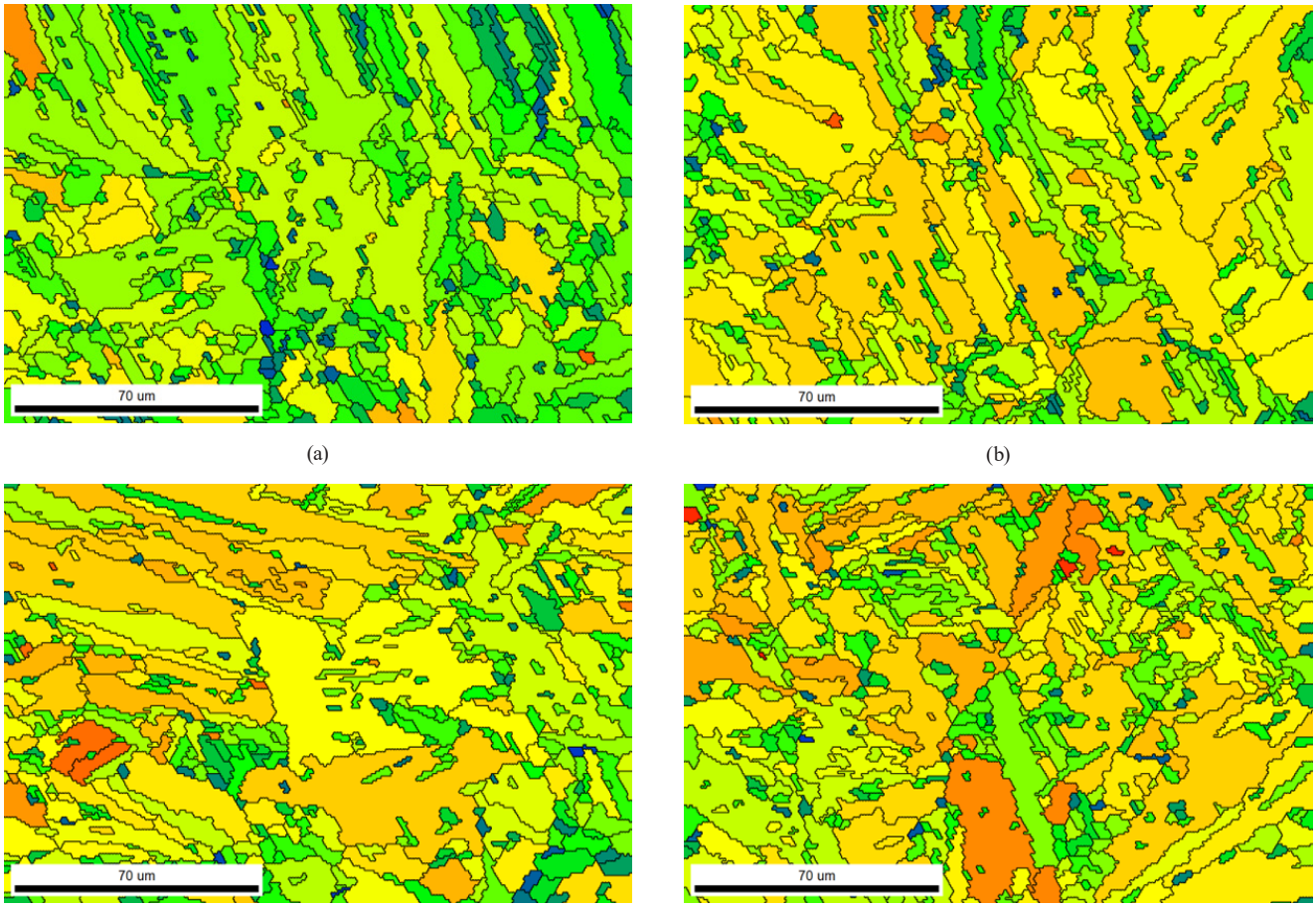

(a) (b)

(c) (d)

Fig. 4 Grain misorientation angle maps of specimens loaded by different tensile forces, (a) $F = 9000$ N, (b) $F = 14000$ N, (c) $F = 19000$ N, (d) $F = 21000$ N

Table 2 Average grain misorientation angles of the elongated specimens

Specimen	1	2	3	4
Grain misorientation angle, degrees	1.156	1.069	1.051	0.887

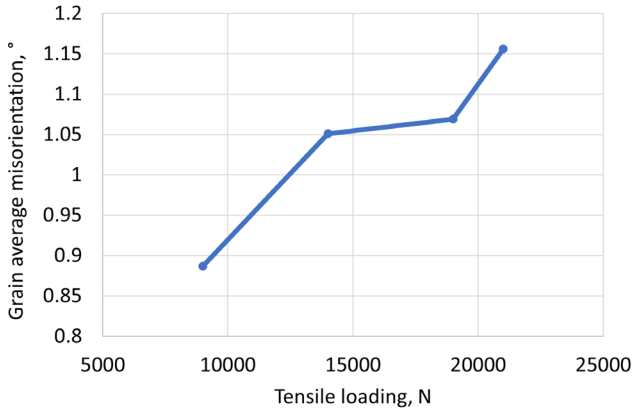

Fig. 5 Grain average misorientation as the function of the applied tensile loading force

4 Conclusions

After quenching the microstructure of the steel showed (lath) martensitic character. This kind of materials is difficult to be deformed plastically, but still shows some plastic behavior. Martensitic transformation itself causes large dislocation density, as it was shown elsewhere [10]. Subsequent plastic deformation can reorganize the dislocation distribution. An overall dislocation density reduction occurs, but the density of the geometrically necessary dislocations increases. Since these dislocations cause a local misorientation in the crystal lattice, the average misorientation between adjacent points within the grains of the material increases. This was proven in this work.

Acknowledgements

The research reported in this paper is part of project no. BME-NVA-02, implemented with the support provided by the Ministry of Innovation and Technology of Hungary

from the National Research, Development and Innovation Fund, financed under the TKP2021 funding scheme. This research work was supported by Ministry of Innovation and Technology of Hungary from the National Research, Development and Innovation Fund OTKA K 124926.

References

[1] Krauss, G. "Martensite in steel: strength and structure", Materials Science and Engineering: A, 273–275, pp. 40–57, 1999. https://doi.org/10.1016/S0921-5093(99)00288-9

[2] Krauss, G., Marder, A. R. "The morphology of martensite in iron alloys", Metallurgical Transactions, 2(9), pp. 2343–2357, 1971. https://doi.org/10.1007/BF02814873

[3] Morito, S. Tanaka, H., Konishi, R., Furuhara, T., Maki, T. "The morphology and crystallography of lath martensite in Fe-C alloys", Acta Materialia, 51(6), pp. 1789–1799, 2003. https://doi.org/10.1016/S1359-6454(02)00577-3

[4] Kitahara, H., Ueji, R., Tsuji, N., Minamino, Y. "Crystallographic features of lath martensite in low-carbon steel", Acta Materialia, 54(5), pp. 1279–1288, 2006. https://doi.org/10.1016/j.actamat.2005.11.001

[5] Swarr, T., Krauss, G. "The Effect of Structure on the Deformation of As-Quenched and Tempered Martensite in an Fe-0.2 Pct C Alloy", Metallurgical Transactions A, 7(1), pp. 41–48, 1976. https://doi.org/10.1007/BF02644037

[6] Michiuchi, M., Nambu, S., Ishimoto, Y., Inoue, J., Koseki, T. "Relationship between local deformation behavior and crystallographic features of as-quenched lath martensite during uniaxial tensile deformation", Acta Materialia, 57(18), pp. 5283–5291, 2009. https://doi.org/10.1016/j.actamat.2009.06.021

[7] Nambu, S., Michiuchi, M., Ishimoto, Y., Asakura, K., Inoue, J., Koseki, T. "Transition in deformation behavior of martensitic steel during large deformation under uniaxial tensile loading", Scripta Materialia, 60(4), pp. 221–224, 2009. https://doi.org/10.1016/j.scriptamat.2008.10.007

[8] Ghassemi-Armaki, H., Chen, P., Bhat, S., Sadagopan, S. Kumar, S., Bower, A. "Microscale-calibrated modeling of the deformation response of low-carbon martensite", Acta Materialia, 61(10), pp. 3640–3652, 2013. https://doi.org/10.1016/j.actamat.2013.02.051

[9] Mine, Y., Hirashita, K., Takashima, H., Matsuda, M., Takashima, K. "Micro-tension behaviour of lath martensite structures of carbon steel", Materials Science and Engineering: A, 560, pp. 535–544, 2013. https://doi.org/10.1016/j.msea.2012.09.099

[10] Szabó, P. J., Field, D. P., Jóni, B., Horky, J., Ungár, T. "Bimodal Grain Size Distribution Enhances Strength and Ductility Simultaneously in a Low-Carbon Low-Alloy Steel", Metallurgical and Materials Transaction A, 46(5), pp. 1948–1957, 2015. https://doi.org/10.1007/s11661-015-2783-x